Journal of the Oceanographical Society of Japan
Vol. 38, pp. 159 to 171, 1982

New Computation of the Wind Stress over the North Pacific Ocean*

Kunio KUTSUWADA**

Abstract: The wind-stress field in the North Pacific Ocean during 1961–75 is computed from nearly five million ship reports. With a drag coefficient having a linear relation to wind speed, annual mean and monthly mean wind-stress fields are obtained, and their features are described.

Compared with the stress fields obtained by HELLERMAN (1967) and WYRTKI and MEYERS (1976), the eastward component of the stress in the present study is larger in magnitude and the northward one smaller in magnitude, especially in the trade wind region. Differences in the drag coefficient do not have a pronounced effect on the estimated stress field. Long-period inter-annual variations in the wind field are the most likely cause of the discrepancies between the present study and those of the above authors.

The maximum of the wind-stress curl, estimated from the annual mean wind-stress fields, is as large as 1.0×10^{-8} dyn cm^{-3} around 30°N, and is larger than that estimated by EVENSON and VERONIS (1975). The discrepancy is considered to be mainly due to differences in the computed stress field itself rather than due to differences in the grid size used in the stress computations.

The Sverdrup transports integrated from the eastern boundary on the basis of the present stress field have a maximum greater than 40×10^{12} cm^3 s^{-1} (Sv.) near the western boundary around 30°N. This value is closer to the observed transport of the Kuroshio than that based on Hellerman's stress field.

1. Introduction

The distribution of wind stress has been used to explain the general features and transports of ocean circulation (SVERDRUP, 1947; MUNK, 1950). Such studies require knowledge of the distribution of the wind-stress curl.

Computations of wind-stress fields over the world ocean were made by HIDAKA (1958) and HELLERMAN (1967, 1968). Recently, WYRTKI and MEYERS (1975, 1976) and BUNKER (1976) computed wind-stress fields in the Pacific Trade wind region and in the North Atlantic, respectively. The studies of the latter two authors are probably better in some aspects than those of the former two authors. First, Hidaka's and Hellerman's computations were based mainly on monthly pilot-chart wind-rose data, while WYRTKI and MEYERS and BUNKER used wind data from ships-of-opportunity. Since wind data obtained on ships-of-opportunity are usually averages for about ten minutes, they may give better estimation of the wind stress than monthly wind-rose data. Secondly, the drag coefficients used by HIDAKA and HELLERMAN are not appropriate. POND and BRYAN (1976) pointed out that the values are too large for strong winds. Thirdly, WYRTKI and MEYERS and BUNKER used smaller grid sizes in the meridional direction than HIDAKA and HELLERMAN. The smaller grid size can yield more detailed features of the stress field, and improve estimations of the wind-stress curl.

Although the stress computation has been improved, there are still some problems to be discussed. First, the determination of the drag coefficient is in dispute. The wind stress computed by using the bulk formula involves inevitable uncertainty for the selection of the drag coefficient. Therefore, it is necessary to examine how differences in the drag coefficient affect the estimation of the stress. Another problem is the selection of grid size. A smaller grid size

* Received Aug. 11, 1981, revised Mar. 26, 1982.
** Ocean Research Institute, University of Tokyo, Minamidai 1-15-1, Nakano-ku, Tokyo, Japan

provides good resolution, while it reduces the reliability in computing the average wind-stress field, because the number of data taken within a grid decreases. We need to have a measure of the reliability of the stress estimation, and to know how the reduction of grid size affects the estimation of wind-stress curl.

In the present study, the mean wind-stress field in the North Pacific Ocean is computed from wind data measured on ships-of-opportunity. The results are compared with the wind-stress fields of HELLERMAN (1967, 1968) and WYRTKI and MEYERS (1975, 1976).

The major purpose of the present study is to establish a more reliable set of data on the wind-stress field in the North Pacific. The data for annual mean and monthly mean stress fields are shown in KUTSUWADA and SAKURAI (1982) along with maps, and are available for other investigators.

2. Data processing

The Japan Meteorological Agency files weather reports from ships-of-opportunity, and nearly five million ship reports during the period 1961 to 1975 were used for the present study. These contain wind observations, ship positions and several meteorological elements such as pressure and air temperature in the North Pacific from the equator to 60°N and from 100°E to 90°W. The units of observations are knots for wind speed and 10-degree increments for wind direction.

In the first data processing, observations which are larger than 55 knots (28 m s^{-1}) in wind speed are rejected, because they can be false. The number of rejected data is less than 2 % of the total. Next, observed wind data are assigned to quadrangles of 2-degrees of latitude by 5-degrees of longitude. For each of the quadrangles, wind stresses are computed based on the bulk method, and their vector averages are calculated both for annual and monthly means.

The number of observations for each quadrangle is shown in Fig. 1. The numbers are relatively large at mid-latitudes, while they decrease toward the lower and higher latitudes. In the eastern part, especially at low latitudes, there are some areas where the numbers of observations are below 20 and the numbers used for the monthly stresses are smaller than 10.

Each ship record was assumed to be observed at about ten meters height, so that the wind stress is computed according to the bulk formula,

$$\vec{\tau}=\rho C_D|\vec{W}|\vec{W} \qquad (1)$$

where $\vec{\tau}$ is wind stress vector, ρ air density, C_D the drag coefficient, and $\vec{W}$ wind vector.

The air density ρ depends mainly on latitude and season. HELLERMAN (1967) used a value for ρ which increases poleward in the northern hemisphere and is independent of month. WYRTKI and MEYERS (1975, 1976) used a constant value, 1.2×10^{-3} g cm^{-3}, considering that

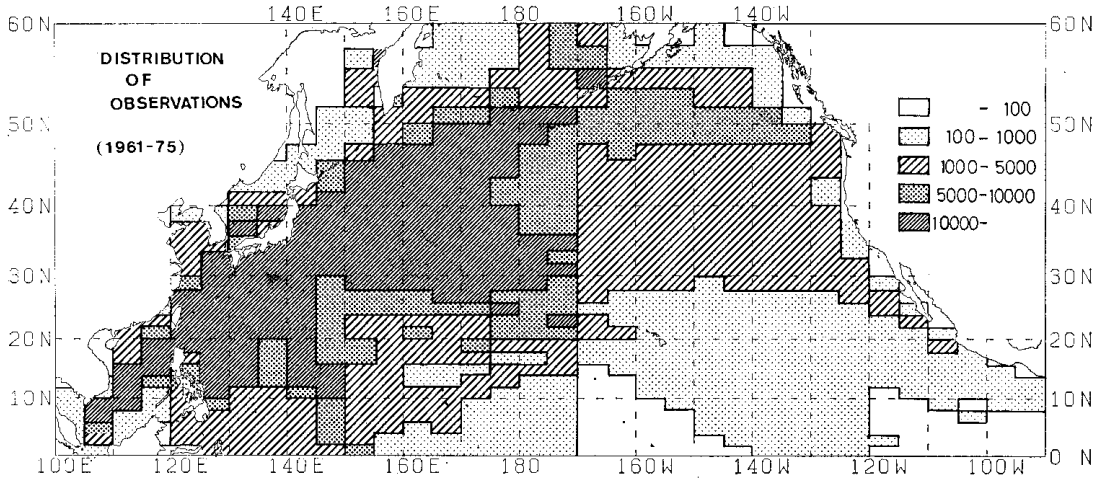

Fig. 1. The distribution of the number of observations for quadrangles of 2-degrees of latitude by 5-degrees of longitude for fifteen years from 1961 to 1975.

the variation of air density in the trade wind region is relatively small. In the present study, ρ is computed from monthly mean sea-level pressure and air temperature data of the Japan Meteorological Agency (1977). These values are averaged zonally for individual month. The monthly averages range from 1.17 to 1.30×10^{-3} g cm^{-3} and are shown in KUTSUWDA and SAKURAI (1982). Differences in ρ from those in HELLERMAN and WYRTKI and MEYERS do not exceed 5%. Moreover, the error due to neglect of the dependency on longitude is $\leqslant 5\%$.

Dependency of the drag coefficient on wind speed under conditions of neutral atmospheric stability have been studied through many field measurements and laboratory experiments, and various relations have been obtained. In HIDAKA (1958)'s computation, C_D was expressed by a step-function of wind speed; there is a transition from low to high values in the vicinity of 7 m s^{-1}. HELLERMAN (1967) also used a drag coefficient

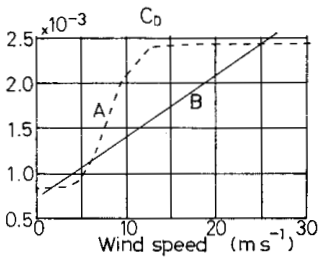

Fig. 2. The dependencies of the drag coefficient in the bulk formula on the wind speed. Broken curve (A): the drag coefficient used in the stress computation by HELLERMAN (1967). Solid curve (B): the drag coefficient used in the present analysis based on GARRATT (1977).

which increases abruptly with wind speed near 7 m s^{-1} (broken curve in Fig. 2). POND and BRYAN (1976) criticized the use of an abrupt increase at a certain specified wind speed, and commented that for strong winds above about 15 m s^{-1} the drag coefficient may be nearly constant or increase slightly with wind speed. On the other hand, WYRTKI and MEYERS (1975, 1976) adopted a constant value, 1.5×10^{-3}, considering that variation of wind speed in the trade wind region is not large.

GARRATT (1977) summarized numerous previous studies on the determination of drag coefficient, and based on results in these studies, he presented the following regression formula,

$$C_D=(0.75+0.067|\vec{W}|)\times 10^{-3} \qquad (2)$$

where $|\vec{W}|$ is the wind speed in m s^{-1}. This drag coefficient which increases linearly with wind speed is shown by the solid line in Fig. 2. The drag coefficient given by Eq. (2) seems to be the most reasonable estimate at present, and hence Eq. (2) is applied to the following computation of wind stress.

3. Annual mean wind-stress field

The annual mean wind-stress field is shown in Fig. 3, and is compared with that of HELLERMAN (1967, 1968). In the present study, stress averages over quadrangles of 2-degrees of latitude by 5-degrees of longitude are obtained, while HELLERMAN computed stresses using 5-degree squares.

Compared with the stress field of HELLERMAN, the present result shows more detailed

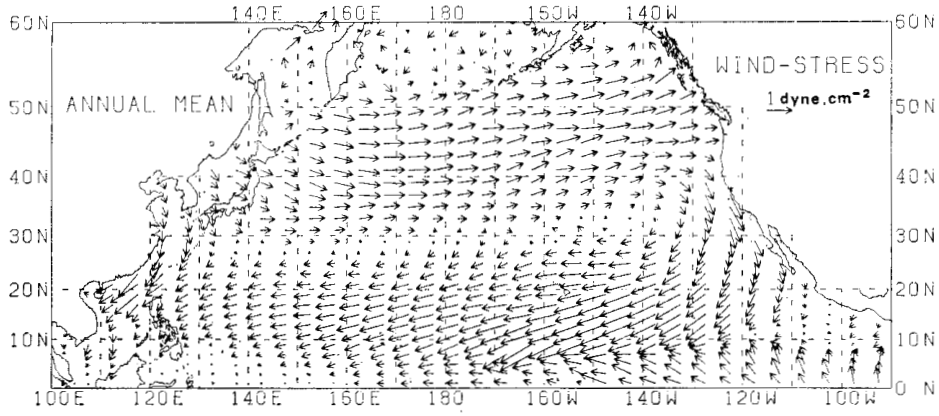

Fig. 3. Annual mean wind stress field.

features in the meridional direction such as the Intertropical Convergence Zone (ITCZ) at eastern low latitudes and the anticyclone around 30°N and 145°W.

Now let us estimate standard errors of the stress components in order to examine reliability of these stress estimations. When there are N wind observations in each grid and the standard deviations of the stress components are σ_x and σ_y, assuming a Gaussian distribution, the standard errors, ε_x and ε_y are given by $\sigma_x/\sqrt{N}$ and $\sigma_y/\sqrt{N}$, respectively. The Gaussian assumption may not entirely valid, as there are probably seasonal variations in the stress components. Nevertheless, as long as discussion is limited to the upper limit of the standard error, the error in this assumption may not be so serious. Since ε_x is nearly equal to or larger than ε_y almost throughout the North Pacific, only the distribution of ε_x is discussed. ε_x depends mainly on the number of observations, and is about 0.02 dyn cm^{-2} in the quadrangles with more than 5,000 observations. ε_x is larger in east of 170°W with decrease of the number of observations, and it does not exceed 0.1 dyn cm^{-2} except for the area near 160°W and south of 15°N. The reliability in the present stress field is about ± 0.1 dyn cm^{-2}.

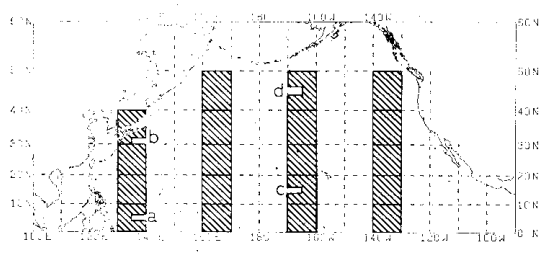

Fig. 4. Test areas used in comparisons between the present stress components and those of Hellerman's. The areas (a), (b), (c) and (d) are used in the computation of Figs. 12 (a), (b), (c) and (d).

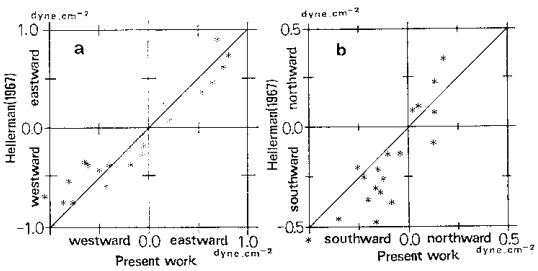

Fig. 5. Comparisons between the present work and Hellerman's of (a): the eastward-, and (b): northward components of average stress in nineteen 10-degree squares shown in Fig. 4.

Comparisons with Hellerman's stress field are made for the test squares (10°×10°) shown in Fig. 4. Figure 5 shows comparisons between the components of our stresses and those of Hellerman's. There are no significant differences for the eastward components (Fig. 5(a)), but the magnitudes of the northward components (b) are generally smaller than Hellerman's. Figure 6 shows that zonal means of the eastward component (a) are larger in magnitude in the region of westward stress than Hellerman's and the northward components (b) are smaller in magnitude for almost all latitudes. Comparison with the stress field by WYRTKI and MEYERS (1975, 1976) is made only for the region south of 30°N. The zonal means of their eastward components seem to be identical with those of HELLERMAN (that is, smaller than ours), while those of their northward components seem to match ours. It should be noted that the dependency of the drag coefficient on wind speed is different in each of these computations. Using different coefficients, stresses in the same areas as in Fig. 5 are recomputed (Fig. 7). In the stresses with a coefficient identical to that of HELLERMAN, the magnitudes of the eastward components (Fig. 7(a)) are larger in the westward-stress region and nearly the same in the eastward-stress region, and those of the northward components (b) show the same features as the eastward ones. On the other hand, the

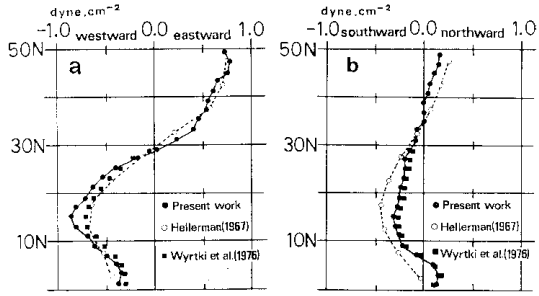

Fig. 6. Meridional profiles of the zonal means of (a): the eastward-, and (b): northward components of annual mean stresses. Black circles are for stresses in the present study, open circles for HELLERMAN (1967)'s and black squares for WYRTKI and MEYERS (1976)'s study.

eastward component of the stresses with the constant C_D also has larger absolute values in the westward-stress region. Thus, it seems that differences in the drag coefficient have little to do with the discrepancies in the stresses.

The discrepancies may be attributable to differences in the period of data sampled. Most of wind data HELLERMAN used were observed in the period before 1962. WYRTKI and MEYERS used wind data during the period 1948 to 1972. On the other hand, the majority of the data used in the present study belong to the period after the early 1960's, and year-to-year variability of the wind stress for fifteen years from 1961 to 1975 was investigated. Figure 8 shows interannual variation of the stresses in the regions where the large divergences from Hellerman's stresses were found. Eastward and northward components of yearly stresses are compared with Hellerman's. In Fig. 8(a) the northward component is smaller in magnitude than Hellerman's throughout the fifteen years, while the eastward one is smaller in magnitude in the early 1960's and larger throughout most of the rest of the period. Thus, the interannual variation tends to show a trend of stronger westward stress with time. Also in Fig. 8(b) the differences in stress components from Hellerman's are rather small

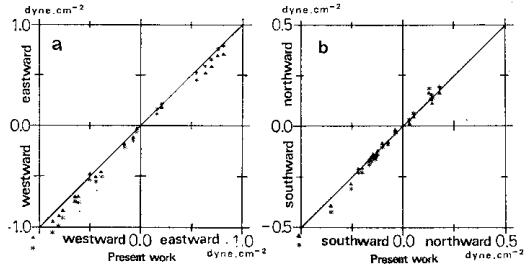

Fig. 7. Comparisons of (a): the eastward- and (b): northward components of average stress in nineteen 10-degree squares shown in Fig. 4 computed by employing different drag coefficients. Stars represent bivariant plots of stresses based on the drag coefficient shown by the solid curve (B) in Fig. 2 against those shown by the broken curve (A) in the same figure, while black triangles are plots of the former stress against the constant value (1.5×10^{-3}).

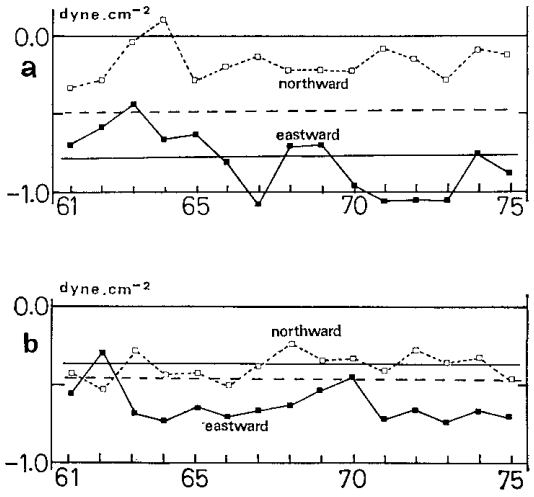

Fig. 8. Time sequences of eastward (solid curve) and northward (broken curve) components of yearly stresses in 10-degree squares (a): 10°–20°N, 170°–160°W; and (b): 20°–30°N, 140°–130°W). Solid and broken horizontal lines represent eastward and northward components of average stress, respectively, from HELLERMAN (1967).

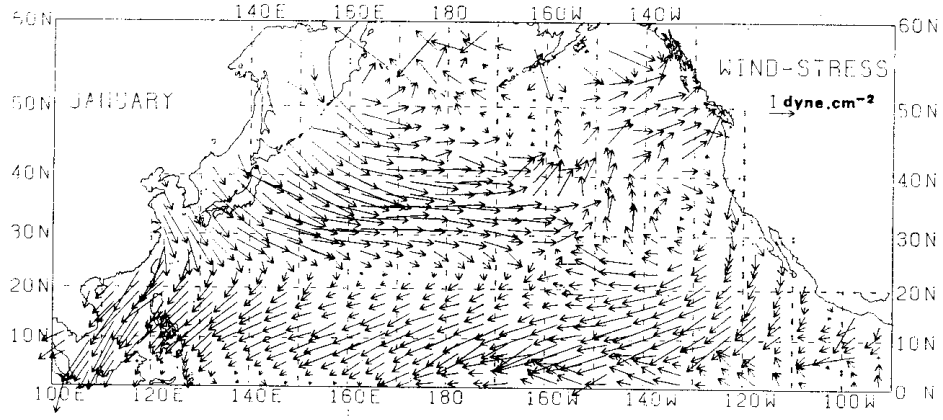

Fig. 9. Wind-stress field for January.

Table 1. Values of the eastward components of mean monthly wind stress over the longitudinal ranges indicated in the last column

Latitude	Ann.	Jan.	Feb.	Mar.	Apr.	May	Jun.	Jul.	Aug.	Sep.
48-50N	71	44	62	70	94	60	30	33	46	71
46-48N	77	58	98	85	89	62	33	29	37	76
44-46N	76	79	118	91	94	61	33	23	25	59
42-44N	65	66	109	94	87	58	30	17	18	41
40-42N	61	94	120	68	65	46	28	18	13	32
38-40N	56	107	132	116	44	40	29	14	11	9
36-38N	53	97	145	114	38	23	22	3	1	5
34-36N	46	125	129	94	13	11	9	−7	−8	−8
32-34N	40	109	124	83	−3	−2	0	−9	−10	−14
30-32N	22	87	106	92	−21	−15	−5	−24	−22	−25
28-30N	2	66	72	31	−37	−24	−10	−36	−35	−29
26-28N	−21	20	26	−1	−49	−38	−19	−54	−40	−39
24-26N	−40	−8	−10	−29	−71	−43	−32	−56	−46	−42
22-24N	−52	−31	−31	−49	−81	−43	−37	−55	−50	−46
20-22N	−63	−44	−58	−62	−94	−63	−49	−56	−54	−45
18-20N	−71	−63	−74	−77	−89	−67	−50	−60	−51	−47
16-18N	−81	−74	−97	−91	−90	−76	−61	−61	−55	−40
14-16N	−86	−88	−113	−105	−99	−86	−71	−58	−47	−36
12-14N	−82	−103	−117	−127	−103	−85	−73	−54	−27	−26
10-12N	−70	−104	−116	−117	−104	−85	−60	−41	−20	−10
8-10N	−63	−111	−112	−116	−89	−66	−45	−23	−10	−8
6- 8N	−50	−94	−83	−99	−72	−43	−34	−19	−20	−6
4- 6N	−40	−66	−59	−76	−44	−32	−27	−30	−28	−17
2- 4N	−36	−55	−49	−42	−35	−33	−33	−44	−40	−25
0- 2N	−38	−41	−41	−29	−30	−37	−33	−37	−43	−40

Table 2. Values of wind-stress curl zonally-averaged over the longitudinal ranges indicated

Latitude	Ann.	Jan.	Feb.	Mar.	Apr.	May	Jun.	Jul	Aug.	Sep.
50N	6	235	134	153	2	−14	37	12	−15	42
48N	33	31	157	88	−6	6	44	−13	−41	14
46N	12	120	97	48	29	9	−2	−20	−42	−64
44N	−47	−50	−46	25	−26	−17	−19	−37	−33	−85
42N	−18	136	76	30	−109	−60	−32	−5	−36	−66
40N	−28	62	66	90	−100	−41	−8	−34	−25	−114
38N	−23	−36	64	−8	−41	−69	−50	−66	−65	−35
36N	−35	142	−66	−87	−126	−69	−67	−62	−58	−72
34N	−36	−46	−1	−48	−101	−87	−62	−48	−39	−43
32N	−77	−101	−60	−139	−84	−65	−37	−82	−63	−43
30N	−95	−82	−139	−99	−94	−61	−38	−85	−75	−35
28N	−110	−206	−204	−149	−61	−66	−48	−86	−29	−45
26N	−88	−124	−166	−129	−108	−29	−66	−18	−31	−14
24N	−65	−110	−97	−104	−74	−24	−41	−13	−34	−27
22N	−53	−54	−124	−63	−18	−95	−62	−6	−17	0
20N	−34	−80	−72	−63	−23	−19	−6	−20	8	−14
18N	−42	−43	−98	−65	−8	−45	−52	−4	−13	34
16N	−22	−59	−67	−65	−40	−46	−48	8	34	12
14N	16	−62	−12	−95	−17	0	−12	8	81	44
12N	57	4	8	47	−2	−5	49	59	40	70
10N	36	−25	24	4	64	79	76	78	56	13
8N	55	81	132	81	77	99	46	21	−33	11
6N	53	130	111	101	128	54	37	−47	−34	−48
4N	21	52	49	153	48	0	−19	−57	−51	−32
2N	−4	71	41	65	24	−17	0	31	−6	−66

zonally-averaged
($\times 10^{-2}$ dyn cm^{-2}).

Oct.	Nov.	Dec.	Jan.	
119	138	116	44	155E to 125W
114	141	143	57	150E to 125W
100	141	151	79	145E to 125W
91	119	122	66	145E to 125W
59	112	142	94	145E to 125W
38	84	124	107	145E to 125W
25	66	116	97	145E to 125W
0	38	103	125	145E to 125W
−16	17	89	109	140E to 120W
−20	−8	54	87	135E to 120W
−30	−27	25	66	130E to 115W
−46	−47	−6	20	139E to 115W
−56	−62	−27	−8	130E to 115W
−64	−76	−58	−31	130E to 110W
−65	−89	−81	−44	130E to 110W
−69	−95	−99	−63	130E to 110W
−70	−106	−121	−74	130E to 110W
−66	−109	−126	−88	130E to 110W
−46	−96	−124	−103	130E to 110W
−30	−70	−120	−104	130E to 110W
−10	−48	−98	−111	130E to 110W
−8	−33	−66	−94	130E to 110W
−22	−27	−60	−66	130E to 110W
−28	−26	−55	−55	130E to 110W
−27	−28	−67	−41	130E to 110W

in the last column ($\times 10^{-10}$ dyn cm^{-3}).

Oc.	Nov.	Dec.	Jan.	
69	90	100	235	155E to 125W
−46	29	127	31	150E to 125W
−56	3	47	120	145E to 125W
−55	−75	−123	−50	145E to 125W
−136	−39	86	136	145E to 125W
−103	−132	−76	62	145E to 125W
−68	−81	−32	−36	145E to 125W
−115	−132	−57	142	145E to 125W
−73	−92	−52	−46	140E to 120W
−14	−118	−156	−101	135E to 120W
−49	−99	−124	−82	130E to 115W
−67	−85	−142	−206	130E to 115W
−42	−63	−95	−124	130E to 115W
−45	−73	−139	−110	130E to 110W
0	−55	−98	−54	130E to 110W
−10	−17	−78	−80	130E to 110W
0	−47	−91	−43	130E to 110W
17	−4	−17	−59	130E to 110W
90	60	11	−62	130E to 110W
80	115	21	4	130E to 110W
93	101	107	−25	130E to 110W
11	69	188	81	130E to 110W
−58	34	35	130	130E to 110W
−24	15	30	52	130E to 110W
3	−6	−51	71	130E to 110W

in the early 1960's, and thereafter the eastward component is often larger in magnitude than Hellerman's and the northward one smaller. These results lead to the conclusion that the stresses may depend, more or less, on the period used for the computation.

4. Monthly mean wind-stress fields

Figure 9 shows the wind-stress field for January and Fig. 10 a distribution of the standard errors ε_x of the eastward components of the stresses for January. In the eastward-stress region north of 30°N the stress magnitudes are largest (about 2.0 dyn cm^{-2}) near 35°N and 160°W, where ε_x exceeds 0.2 dyn cm^{-2}. In the westward-stress region, the stress magnitudes are largest (about 2.0 dyn cm^{-2}) near 8°N and 155°W, where ε_x exceeds 0.3 dyn cm^{-2} due to the poor data coverage.

It is difficult to determine an upper limit of the standard error appropriate for description of the monthly mean stress field. If we choose 0.1 dyn cm^{-2} as the upper limit of error, about half of the present computations for the North Pacific are rejected (see Fig. 10), because to reduce the error to this size requires at least 1,000 wind observations for each quadrangle. If 0.2 dyn cm^{-2} is selected as the upper limit, some small areas around 160°W, where only 200 or less observations are available, must be rejected. But, for this upper limit, it is possible to include these areas by using a larger grid size. For example, in the case of stresses in quadrangles of 4-degrees of latitude by 5-degrees of longitude, the values of ε_x in Fig. 10 decrease by 20 to 30 %.

Zonal means of the eastward component of the monthly mean stresses are given in Table 1. Figure 11 depicts their meridional profiles for

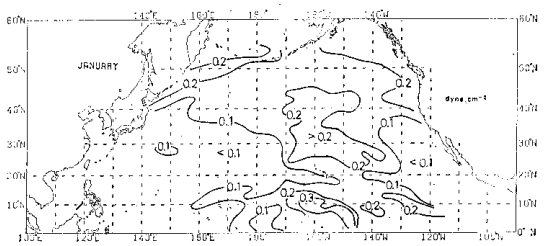

Fig. 10. The distribution of standard errors of the eastward components of wind stress for January. Units are dyn cm^{-2}.

each month, which are compared with those for the annual mean. The zonal means south of 30°N in Table 1 are about 10% larger than those of WYRTKI and MEYERS (1976) throughout the year.

Seasonal variations of the stresses in some representative areas are shown in Figs. 12 along with their standard errors. In the tropical monsoon region (Fig. 12(a)), the stress direction is southwestward from October to April and nearly reverses to northeastward for the rest of the year. In the temperate monsoon region (Fig. 12(b)), a southeastward stress is dominant from November to March, while a northward or northwestward one dominates from May to August. The standard errors in Figs. 12(c) and (d) exceed 0.1 dyn cm^{-2} for most of the year. In both of the areas, the eastward component is dominant throughout the year. In Fig. 12(c) (northeast trade wind region) the westward component has a maximum in magnitude in March and a minimum in October, while in Fig. 12(d) (westerly wind region) the eastward component is large in March and in October.

5. Wind-stress curl and the Sverdrup transport fields

The curl of the wind stress was computed

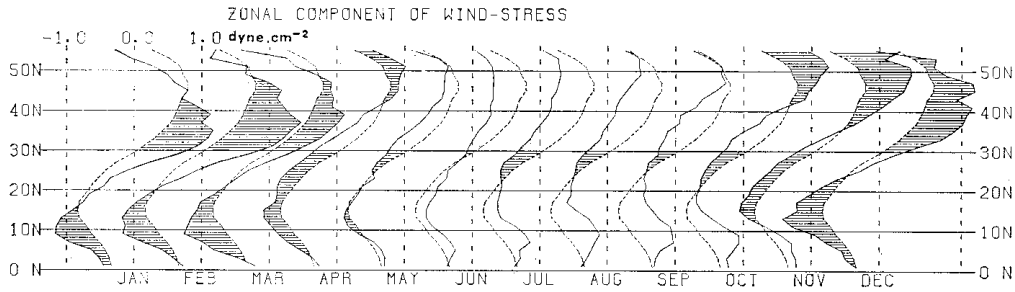

Fig. 11. The annual cycle of meridional profiles of the eastward components of wind stress zonally-averaged over the range indicated in the last column of Table 1. Solid and broken curves show eastward components of the wind stress for monthly and annual means, respectively. Units are 1.0 dyn cm^{-2}. Shaded zones indicate monthly mean values of wind stress larger in magnitude than the annual means.

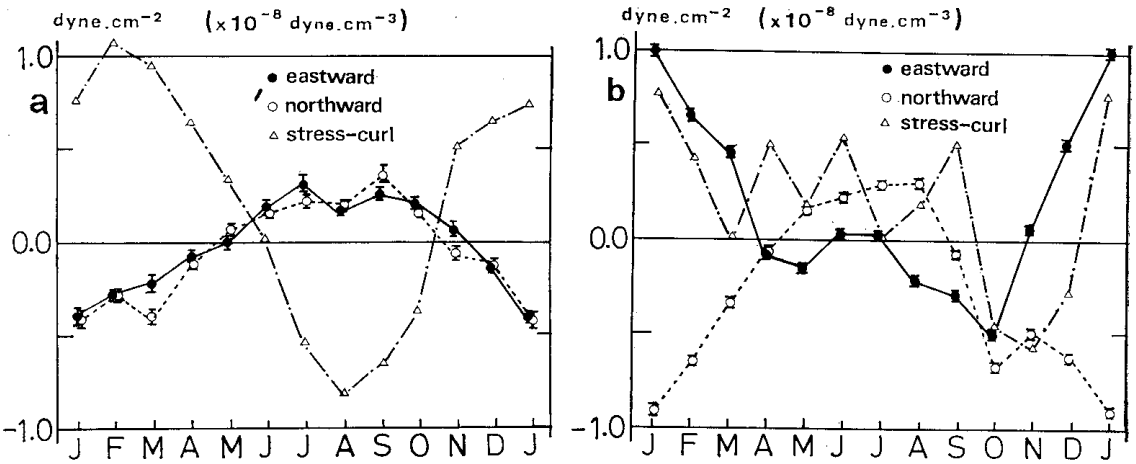

Fig. 12. Seasonal variations of eastward (black circles) and northward (open circles) components and wind stress curl (triangles) in (a): the tropical monsoon region (4°N-6°N, 135°E-140°E); (b): the temperate monsoon region (30°-32°N, 135°-140°E); (c): the northeast trade wind region (14°-16°N, 170°-165°W); and (d): the westerly wind region (44°-46°N, 170°-165°W). Vertical bars indicate standard errors in the estimation of monthly stresses.

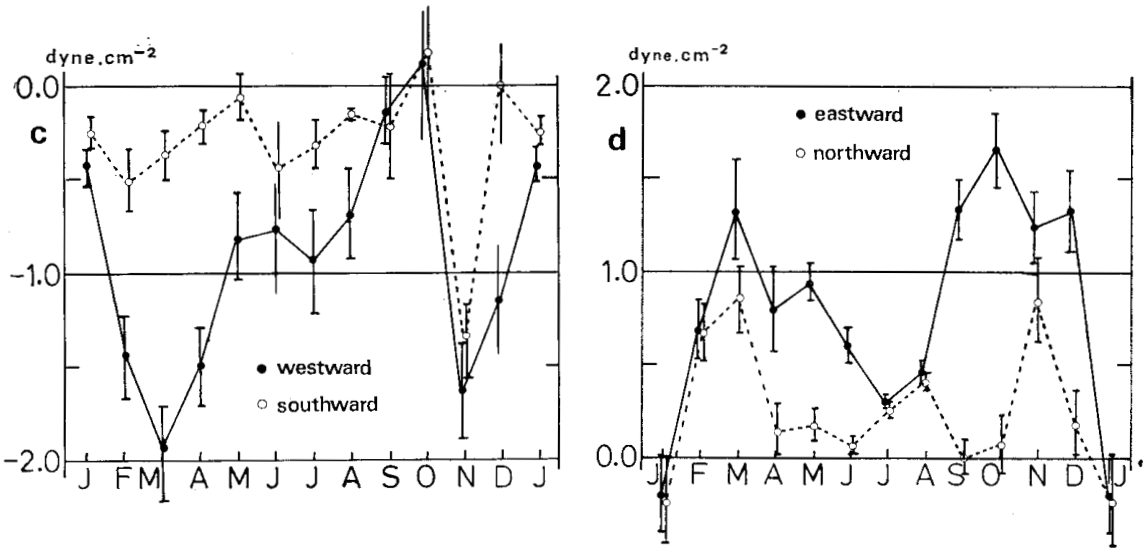

Fig. 12. (continued)

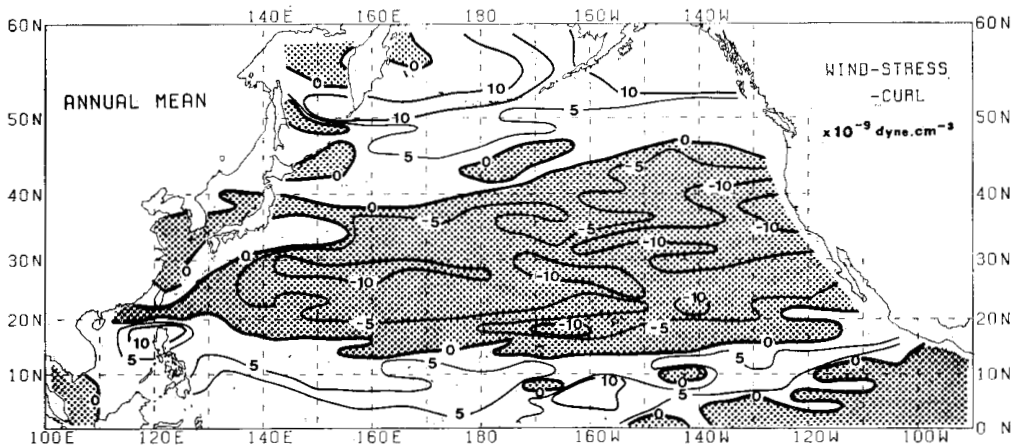

Fig. 13. The isopleths of wind stress curl computed from the annual mean wind-stress fields. The shaded area indicates negative curl (anticyclonic vorticity), while the rest is positive (cyclonic vorticity).

according to,

$$\mathrm{curl}_z \vec{\tau} = \frac{\partial \tau_y}{\partial x} - \frac{\partial \tau_x}{\partial y} \qquad (3)$$

where τ_x is the eastward component of the stress and τ_y the northward component. For each of the intersections of the $2° \times 5°$ grid except those in areas near the boundaries, the curl of the stress is calculated. The meridional volume transport V is estimated in the interior region of the ocean, by applying the above values of the curl to the following Sverdrup relation,

$$\beta V = \mathrm{curl}_z \vec{\tau} \qquad (4)$$

where β is the latitudinal derivative of the Coriolis parameter.

Figure 13 shows contours of wind-stress curl estimated from the annual mean wind-stress field. The latitude of the northern boundary of the negative curl region becomes higher toward the east. West of 160°E the region with positive curl occupies the region to the south of Japan. This feature is also found in the North Atlantic (LEETMAA and BUNKER, 1978). However, this feature is not evident in the curl field of EVENSON and VERONIS (1975) who

used HELLERMAN (1967)'s wind-stress field. Maximum values of the negative curl occur around 30°N and are as large as 1.0×10^{-8} dyn cm^{-3}. The values are 20 to 30% larger than those given by EVENSON and VERONIS (1975).

It is possible that the estimation of the curl is affected by the grid size. SAUNDERS (1976) estimated the curl on 1-degree squares over the North Atlantic, and pointed out that the curl on a coarse spatial resolution can be underestimated. It should be noted that the grid size we used (2°×5°) is smaller in the meridional direction than that of HELLERMAN (1967) (5°×5°). Stresses and values of the curl were also estimated in larger quadrangles (4°×5°), and Fig. 14 shows the meridional profile of their zonal means as well as that for the finer grid (2°×5°). The maximum differences between the present results and those of EVENSON and VERONIS (1975) (based on Hellerman's stress field) are as large as 0.3×10^{-8} dyn cm^{-3}. On the other hand, the differences for the larger grid size are $\sim0.1\times10^{-8}$ dyn cm^{-3} or smaller.

Seasonal variations of the stress curl are shown in Figs. 12(a) and (b), while they are not shown in Figs. 12(c) and (d) because the standard errors are large. In the tropical monsoon region (Fig. 12(a)), there is a pronounced seasonal variation, which has a cyclonic curl during the period with southwestward stress and an anticyclonic one during the period with northeastward stress. In the temperate monsoon region south of Japan (Fig. 12(b)), the cyclonic curl persists from January to September, and the anticyclonic curl from October to December. Table 2 shows zonal means of the curl estimated from monthly wind stress. The anticyclonic curl region exists at mid-latitudes, and has a maximum value larger than 2.0×10^{-8} dyn cm^{-3} near 28°N in winter, while in summer it moves northward and the values reach to their smallest. The cyclonic curl region at low latitudes also has a maximum in winter and a minimum in summer.

Figure 15 shows contours of the Sverdrup transport integrated westward from the eastern boundary along lines of latitude. The transport

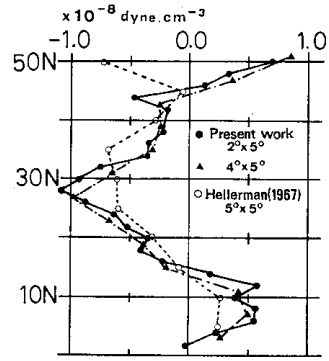

Fig. 14. Meridional profiles of the zonal means of wind stress curl. Black circles represent means estimated on a 2°×5° grid and black triangles on a 4°×5° grid, while open circles are based on Hellerman's stress field. Units are 10^{-8} dyn cm^{-3}.

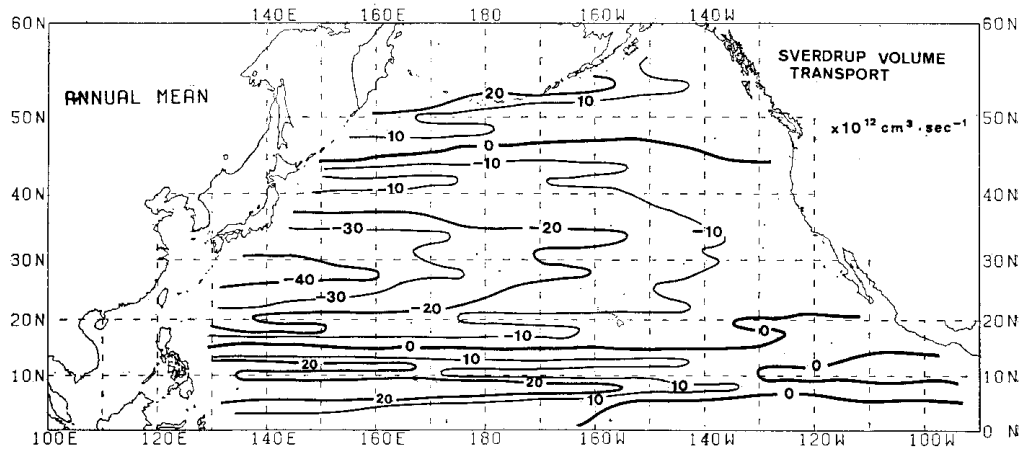

Fig. 15. The isopleths of the meridional Sverdrup volume transports integrated westward along each line of latitude from the eastern boundary. Positive values show northward transports and negative values southward transports.

stream function is taken to be zero along the eastern boundary. The negative curl region indicates southward volume transport. Supposing mass conservation for the transports shown in Fig. 15, we can evaluate the transports of the western boundary currents as the return flow of their integrated values across the full width of the ocean for each latitude. Figure 15 shows a maximum value larger than 40×10^{12} cm^3 s^{-1} (Sv.) at the western boundary near 30°N. This value is also larger than that reported by EVENSON and VERONIS (1975) (about 30 Sv.), and is closer to the observed transports in the Kuroshio (see Appendix).

6. Discussion and summary

The main purpose of the present study has been to establish a data set on the surface wind-stress field of the North Pacific which will contribute to dynamical studies of the oceanic circulation in this region of the Pacific Ocean. Both the annual and the monthly means stresses in $2°\times5°$ quadrangles have been computed.

It was found in Section 3 that the stress field in the present study differs in some respects from those of HELLERMAN (1967, 1968) and of WYRTKI and MEYERS (1975, 1976), and these differences could not be accounted for by differences in the drag coefficient. The computation of wind stress contains some inevitable sources of error, many of which were discussed by LEETMAA and BUNKER (1978). One of them lies in the original wind data. It seems that wind speeds observed by merchant ships tend to be larger than those observed by weather ships. The heights of the anemometer differ among ships, perhaps depending on the size of the ships. These error sources may affect the magnitude of computed stresses and the stress components equally. However, the differences between the present results and those of HELLERMAN showed that the eastward component is larger in magnitude while the northward one is smaller (see Figs. 6). Thus, the differences are probably not due mainly to errors in the observed winds.

Another large source of error lies in the uncertainty in the value of the drag coefficient. The error is not only due to the dependency of the coefficient on wind speed discussed in Section 3, but also due to atmospheric stratification. DEARDORFF (1968) demonstrated that the drag coefficient is smaller in the stable state than in the neutral state, while it is larger in the unstable one. The sea-minus-air temperature gives a good measure of atmospheric stability. According to the Japan Meteorological Agency (1977), sea-minus-air temperature has a maximum larger than 7 degrees around Japan in January. Application of DEARDORFF(1968)'s relation under this condition yields a value for the drag coefficient that is 15% larger than in neutral conditions. On the other hand, in the center of the trade wind region where the large difference from Hellerman's results was found, the temperature difference between the sea and air does not exceed 1.5 degrees throughout the year. This implies that the deviation of the drag coefficient from the neutral value is at most 10%, and hence neglect of atmospheric stratification may not account for the discrepancies. The present analyses seem to indicate that the discrepancies have something to do with long-term variations in the atmosphere. This may be found in a time sequence of the original wind data rather than from the computed with stresses.

In the estimation of the stress curl, the results in the present study are larger than those of EVENSON and VERONIS (1975), which were estimated from Hellerman's stresses. It is concluded that this is mainly due to differences in the estimation of the stress rather than differences in grid size.

Knowledge of time and space variabilities of the wind stress are necessary for investigating the response of the ocean to atmospheric forcing. The present study can supply such studies with a useful data set, and besides, be extended to the study of interannual variations.

Acknowledgement

The author wishes to express his great appreciation to Profs. T. TERAMOTO and T. ASAI for encouraging and giving advice during this study. Thanks are extended to Prof. N. SUGINOHARA and Drs. K. TAKEUCHI and M. FUKASAWA for reading the manuscript and making helpful comments. He is much indebted to the Marine Department of the Japan Meteorological Agency for kindly supplying the data used in this study.

Appendix

〈Comparisons of estimated with observed transports〉

It is possible to compare the estimated transports in Section 5 with observed ones. However, most of the observed transports depend on the assumed level of no motion. NITANI (1975) showed that the transports of the Kuroshio referred to 1,000 db off Enshû-nada and off Shiono-misaki vary between 30 and 90 Sv. and their average is about 60 Sv. He also showed that, when a deeper level of no motion was adopted, the Kuroshio transport would increase. It may be that the level of no motion in the Kuroshio is not shallower than 1,000 db. Thus, the transport (larger than 40 Sv.) estimated in Section 5 is closer to the observed one than that (about 30 Sv.) obtained from the stresses of HELLERMAN.

It seems that the transport or the surface velocity in the Kuroshio has a maximum in summer and a minimum in autumn or winter (MASUZAWA, 1965; TSUCHIDA, 1971; TAFT, 1972; MINAMI *et al.*, 1979). These results suggest seasonal variations in the baroclinic current. However, since the time scale of the baroclinic response of the ocean to wind at mid-latitudes is much larger than a year (VERONIS and STOMMEL, 1956), the comparison of estimated and observed transports is not valid. The time scale of oceanic response to the wind is known to be a function of latitude, and becomes smaller toward the equator (LIGHTHILL, 1969). Thus, comparisons for equatorial current systems may be valid. Comparison was made for the Mindanao Current, which is the western boundary current in the tropical gyre and flows southward around 8°N along the east coast of Mindanao Island. Maximum values of the transports in the tropical gyre based on the stress field presented here also showed seasonal variation. They were larger (about 40 Sv.) from winter to late spring, and smaller (20 to 30 Sv.) from late summer to autumn. Some early observations showed a winter maximum for the Mindanao Current (SCHOTT, 1939; WYRTKI, 1961: chap. 3), but MASUZAWA (1969) found no clear difference between summer and winter. Due to the paucity of the observed data, these studies can not yield the synoptic features of seasonal variation in the Mindanao Current. Moreover, recent works (MASUZAWA and NAGASAKA, 1975; KUTSUWADA, in preparation) indicate the existence of interannual variations in the northwestern tropical Pacific that are larger in amplitude than seasonal variations. In order to clearly establish this point, however, we need systematic observations.

References

BUNKER, A. F. (1976): Computations of surface energy flux and annual air-sea interaction cycles of the North Atlantic Ocean. Mon. Wea. Rev., **104**, 1122-1139.

DEARDORFF, J. W. (1968): Dependence of air-sea transfer coefficient on bulk stability. J. Geophys. Res., **73**, 2549-2557.

EVENSON, A. J. and G. VERONIS (1975): Continuous representation of wind stress and wind stress curl over the world ocean. J. Mar. Res., **33** (Suppl.), 131-144.

GARRATT, J. R. (1977): Review of drag coefficients over oceans and continents. Mon. Wea. Rev., **105**, 915-929.

HIDAKA, K. (1958): Computation of the wind stresses over the oceans. Rec. Oceanogr. Wks. Japan, **4**, 77-123.

HELLERMAN, S. (1967): An updated estimate of the wind stress on the world ocean. Mon. Wea. Rev., **95**, 607-614.

HELLERMAN, S. (1968): Correction. Mon. Wea. Rev., **96**, 63-74.

JAPAN METEOROLOGICAL AGENCY, MARINE DEPARTMENT. (1977): Marine climatological tables of the North Pacific Ocean for 1961-1970. Japan Meteorological Agency, Tokyo, 188 pp.

KUTSUWADA, K. and K. SAKURAI (1982): Climatological maps of wind stress field over the North Pacific Ocean. Oceanogr. Mag., **32**, 25-46.

LEETMAA, A. and A. F. BUNKER. (1978): Updated charts of the mean annual wind stress, convergences in the Ekman Layers and the Sverdrup transports in the North Atlantic. J. Mar. Res., **36**, 311-322.

LIGHTHILL, M. J. (1969): Dynamic response of the Indian Ocean to onset of the Southwest Monsoon. Phil. Trans. Roy. Soc. London, **A265**, 45-92.

MASUZAWA, J. (1965): A short note of seasonal variation of the current velocity of the Kuroshio. J. Oceanogr. Soc. Japan, **21**, 117-118 (in Japanese).

MASUZAWA, J. (1969): The Mindanao Current. Bull. Jap. Soc. Fish. Oceanogr., Special Number Prof. Uda's Commemorative Papers, 99-104 (in Japanese with English abstract).

MASUZAWA, J. and K. NAGASAKA (1975): The

137°E oceanographic section. J. Mar. Res., **33**, 109-116.

MINAMI, H., E. KAMIHIRA, K. KOMURA, H. EGUCHI and J. NISHIZAWA (1979): Statistical features of the oceanographic conditions south of Honshu, Japan. (Part 2: In spring and autumn off Kii Peninsula). Bull. Kobe Mar. Obs., **197**, 1-11 (in Japanese with English summary).

MUNK, W. H. (1950): On the wind-driven ocean circulation. J. Meteor., **7**, 79-93.

NITANI, H. (1975): Variation of the Kuroshio south of Japan. J. Oceanogr. Soc. Japan, **31**, 154-173.

POND, S. and K. BRYAN (1976): Numerical models of the ocean circulation. Rev. Geophys. and Space Phys., **14**, 243-263.

SAUNDERS, P. M. (1976): On the uncertainty of wind stress curl calculations. J. Mar. Res., **34**, 155-160.

SCHOTT, G. (1939): Die äquatorialen Stromungen des westlichen Stillen Ozens. Ann. Hydrogr. Berl., **67**, 247-257.

SVERDRUP, H. V. (1947): Wind-driven currents in a baroclinic ocean; with application to the equatorial currents of the eastern Pacific. Proc. Nat. Acad. Sci. Wash., **33**, 318-326.

TAFT, B. A. (1972): Characteristics of the flow of the Kuroshio south of Japan. *In*, Kuroshio—Its Physical Aspects, ed. by H. STOMMEL and K. YOSHIDA, Univ. Tokyo Press, Tokyo, pp. 165-216.

TSUCHIDA, T. (1971): On the seasonal variation of the Kuroshio southeast of Yakushima Island. Oceanogr. Mag., **23**, 1-10.

VERONIS, G. and H. STOMMEL (1956): The action of variable wind stresses on a stratified ocean. J. Mar. Res., **15**, 43-75.

WYRTKI, K. (1961): Physical Oceanography of the Southeast Asian Waters. Scientific results of marine investigations of the South China Sea and the Gulf of Thailand, 1959-1961. Naga Report, **2**, 195 pp.

WYRTKI, K. and G. MEYERS (1975): The trade wind field over the Pacific Ocean. Part I. The mean field and the mean annual variation. Hawaii Inst. Geophys. Rep., HIG-75-1, Univ. Hawaii, 26 pp.

WYRTKI, K. and G. MEYERS (1976): The trade wind field over the Pacific Ocean. J. Appl. Meteor., **15**, 698-704.

北太平洋上の風の応力の再評価

礒　田　邦　夫*

要旨: 1961-75 の15年間の船舶報告約500万個を用いて北太平洋上の風の応力計算を行なった．抵抗係数は風速の1次関数で与え，年平均場及び月平均場を得て，それらの特徴を記述した．従来計算された応力場 (HELLERMAN, 1967; WYRTKI and MEYERS, 1976) に比較して，応力の東西成分が大きく南北成分が小さいという相違がみられ，特に貿易風域でその差が大である．抵抗係数の相違は応力の計算結果に顕著な影響をもたらさない．応力場の比較にみられる相違はデータ・ソースの時期の相違が主要因と考えられ，海上風の場における長周期経年変動の存在を示唆する．

年平均応力場から算出した応力のカールは 30°N 付近で 1.0×10^{-8} dyn cm^{-3} の最大値を示し，EVENSON and VERONIS (1975) による同様な評価を上回る．この相違は応力計算に用いられた桝目の大きさよりは応力場自体に存在する相違に起因すると考えられる．

本応力計算に基く Sverdrup Transport の東岸からの積分値は，30°N 付近の西岸で 40×10^{12} cm^3 s^{-1} (Sv.) 余りを示し，HELLERMAN の応力場に基く同様な評価よりも黒潮の観測値に近い．

* 東京大学海洋研究所　海洋物理部門
〒164 東京都中野区南台1-15-1